J|A|C|S
ARTICLES
Published on Web 12/09/2003

A Nonempirical Anisotropic Atom−Atom Model Potential for Chlorobenzene Crystals

Graeme M. Day† and Sarah L. Price*

Contribution from the Department of Chemistry, University College London, 20 Gordon Street, London, WC1H 0AJ, United Kingdom

Received September 5, 2003; E-mail: s.l.price@ucl.ac.uk

Abstract: A nearly nonempirical, transferable model potential is developed for the chlorobenzene molecules ($C_6Cl_nH_{6-n}$, $n = 1$ to 6) with anisotropy in the atom−atom form of both electrostatic and repulsion interactions. The potential is largely derived from the charge densities of the molecules, using a distributed multipole electrostatic model and a transferable dispersion model derived from the molecular polarizabilities. A nonempirical transferable repulsion model is obtained by analyzing the overlap of the charge densities in dimers as a function of orientation and separation and then calibrating this anisotropic atom−atom model against a limited number of intermolecular perturbation theory calculations of the short-range energies. The resulting model potential is a significant improvement over empirical model potentials in reproducing the twelve chlorobenzene crystal structures. Further validation calculations of the lattice energies and rigid-body $\mathbf{k} = 0$ phonon frequencies provide satisfactory agreement with experiment, with the discrepancies being primarily due to approximations in the theoretical methods rather than the model intermolecular potential. The potential is able to give a good account of the three polymorphs of *p*-dichlorobenzene in a detailed crystal structure prediction study. Thus, by introducing repulsion anisotropy into a transferable potential scheme, it is possible to produce a set of potentials for the chlorobenzenes that can account for their crystal properties in an unprecedentedly realistic fashion.

Introduction

While most of chemistry focuses on the behavior of the valence electrons, the computer modeling of molecular recognition processes, such as the formation of liquids and crystals or biomolecular complexes, usually assumes that molecules interact as if they were a superposition of spherical atomic charge distributions. Considerable progress and understanding has come from computer simulations using the isotropic atom−atom model intermolecular potential.[1,2] However, as we demand more quantitative accuracy from computer simulations, over a greater range of properties, the limitations of this assumption for certain interactions are becoming well-established.[3,4] The most orientation-dependent term in the interaction between most organic molecules, the electrostatic energy, is increasingly being represented by either sets of atomic multipoles or additional off-nuclear charges, to represent the effects of the anisotropic distribution of lone pair and π-electron density on the directionality of hydrogen bonding and $\pi-\pi$ interactions.[5,6] However, given that the valence electron density is generally not spherically distributed about the nuclei in molecules, this anisotropy should, in principle, also affect the other terms in the atom−atom description of the intermolecular potential.[3]

Interactions with chlorine, as well as the heavier halogens, clearly show anisotropic intermolecular interactions; C−Cl···Cl−C close intermolecular contacts are typically 0.2 Å shorter for head-on than side-on contacts.[7,8] It has been debated as to whether the orientation dependence of Cl···Cl interactions is due to a specific attractive force or anisotropy in the repulsive wall, arising from the valence electron distribution.[8−10] Intermolecular perturbation theory (IMPT)[11−13] calculations on chloromethane dimers[8] demonstrate that the interaction is dominated by exchange−repulsion, electrostatic, and dispersion contributions, the first two of which contribute most to the orientational anisotropy. This anisotropy in the repulsive wall has not been included in the many attempts[14−19] to derive an isotropic atom−atom model potential for describing the crystal

† Current address: Department of Chemistry, University of Cambridge, Lensfield Road, Cambridge, CB2 1EW, United Kingdom.

(1) Pertsin, A. J.; Kitaigorodskii, A. I. *The Atom-Atom Potential Method. Applications to Organic Molecular Solids*; Springer-Verlag: Berlin, 1987.
(2) Gavezzotti, A., Ed. *Theoretical Aspects and Computer Modeling of the Molecular Solid State*; John Wiley & Sons: Chichester, 1997.
(3) Stone, A. J.; Price, S. L. *J. Phys. Chem.* **1988**, *92*, 3325.
(4) Stone, A. J. *The Theory of Intermolecular Forces*; Oxford University Press: Oxford, 1996.
(5) Price, S. L. *J. Chem. Soc., Faraday Trans.* **1996**, *92*, 2997.
(6) Price, S. L. In *Reviews in Computational Chemistry*; Lipkowitz, K. B., Boyd, D. B., Eds.; Wiley-VCH: John Wiley & Sons: New York, 2000; Vol. 14, pp 225−289.
(7) Nyburg, S. C.; Faerman, C. H. *Acta Crystallogr.* **1985**, *B41*, 274.
(8) Price, S. L.; Stone, A. J.; Lucas, J.; Rowland, R. S.; Thornley, A. E. *J. Am. Chem. Soc.* **1994**, *116*, 4910.
(9) Ramasubbu, N.; Parthasarathy, R.; Murray-Rust, P. *J. Am. Chem. Soc.* **1986**, *108*, 4308.
(10) Desiraju, G. R.; Parthasarathy, R. *J. Am. Chem. Soc.* **1989**, *111*, 8725.
(11) Hayes, I. C.; Stone, A. J. *Mol. Phys.* **1984**, *53*, 83.
(12) Hayes, I. C.; Stone, A. J. *Mol. Phys.* **1984**, *53*, 69.
(13) Stone, A. J. *Chem. Phys. Lett.* **1993**, *211*, 101.
(14) Bonadeo, H.; D'Alessio, E. *Chem. Phys. Lett.* **1973**, *19*, 117.
(15) Bates, J. B.; Busing, W. R. *J. Chem. Phys.* **1974**, *60*, 2414.
(16) Reynolds, P. A.; Kjems, J. K.; White, J. W. *J. Chem. Phys.* **1974**, *60*, 824.
(17) Mirsky, M.; Cohen, M. D. *Chem. Phys.* **1978**, *28*, 193.
(18) Hsu, L.-Y.; Williams, D. E. *Acta Crystallogr.* **1980**, *A36*, 277.
(19) van Eijck, B., P. *Phys. Chem. Chem. Phys.* **2002**, *4*, 4789.

10.1021/ja0383625 CCC: $25.00

packings of the chlorobenzene series of molecules. These model potentials are unable to reproduce all the structures and close intermolecular contacts satisfactorily across the series. This is consistent with the results of an analysis of the three polymorphs of *p*-dichlorobenezene,[20] which concluded that Cl···Cl anisotropy is sufficiently important to the crystal packing, thermal expansion, and vibrational properties that the isotropic atom−atom form cannot result in a generally transferable model.[21]

Although the crystal structures of chlorinated hydrocarbons show evidence of repulsion anisotropy, deriving a quantified anisotropic potential by empirical parametrization is likely to be an ill-defined fitting problem and less convincing than a nonempirical derivation from the molecular charge distribution. A method of quantifying analytical anisotropic atom−atom repulsion potentials is being developed for organic molecules by assuming that the short-range repulsive contributions are proportional to the overlap of the charge distributions. Application to molecular chlorine[22] and chlorothalonil ($C_6Cl_4(CN)_2$)[23] show the expected form of anisotropy, with greater repulsion in the directions of the lone pair density. An alternative model for this anisotropy,[24] with ellipsoidal chlorine atoms, reproduces the room temperature structure of hexachlorobenzene slightly better than the most successful isotropic model,[18] as well as giving fairly good values of the thermal expansion. However, a recent extension of this model to *p*-dichlorobenzene[25] uses a different atomic shape for the chlorine atoms, indicating possible problems with the transferability of the model.

This work aims to derive an anisotropic atom−atom model potential for the chlorobenzenes, using a nearly nonempirical approach based on the molecular charge distribution. The methodology allows some evaluation of the accuracy of transferring the repulsion−dispersion between the different chlorobenzene molecules. The model potential is first tested on its ability to reproduce the crystal structures of the chlorobenzene family. The Supporting Information demonstrates how these crystal structures are used to distinguish between some sets of plausible assumptions in the model development, particularly in the dispersion coefficients. The accuracy and transferability of the model potential is further tested by calculating the lattice energies, phonon frequencies, and thermodynamic properties. Finally, since the recent resurgence of interest in deriving accurate models for organic intermolecular interactions has been driven by the accuracy required for crystal structure prediction,[26−31] we test the final model potential for its ability to predict the three polymorphs of *p*-dichlorobenzene. These polymorphs represent a stringent test of the model potential because the structures sample several orientations of Cl···Cl contacts where the Cl atoms are in identical chemical environments, and the sluggish nature of the phase changes[32,33] has allowed extensive experimental data to be determined on all three forms at the same temperature. The unprecedented range of properties that can be modeled by the final model potential for chlorobenzenes suggests that considerable realism can be obtained for transferable atomistic model potentials provided that the anisotropy of the valence electron distribution is appropriately represented.

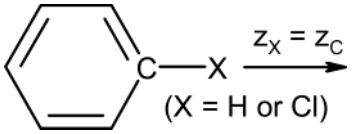

Figure 1. Definition of atomic axes.

Methods

The transferable model potential for the chlorobenzenes comprises of an anisotropic atom−atom model for the electrostatic interactions and the short-range repulsion, plus an isotropic atom−atom model for dispersion; i.e.,

$$U = \sum_{i\in\mathrm{M},k\in\mathrm{N}} [A^{\iota\kappa} \exp(-\alpha^{\iota\kappa}[R_{ik} - \rho^{\iota\kappa}(\Omega_{ik})]) - C_6^{\iota\kappa}/R_{ik}^6 + U_{\mathrm{elec}}(\mathrm{DMA},\Omega_{ik},R_{ik}^{-n},n \le 5)] \quad (1)$$

where R_{ik} is the interatomic separation between atoms i and k of type ι and κ in molecules M and N, respectively. Ω_{ik} represents the relative orientation of the atoms, and the function $\rho^{\iota\kappa}(\Omega_{ik})$ describes anisotropy in the atom−atom repulsion, modifying the exponential decay of this term. We express $\rho^{\iota\kappa}(\Omega_{ik})$ in terms of the scalar products of the unit interatomic vector $\hat{\mathbf{R}}_{ik}$ and the unit intramolecular atomic vectors $\hat{\mathbf{z}}_i$ and $\hat{\mathbf{z}}_k$, as defined in Figure 1. The most appropriate form was found to be

$$\rho^{\iota\kappa}(\Omega_{ik}) = \rho_0^{\iota\kappa} + \rho_1^{\iota}(\hat{\mathbf{z}}_i \cdot \hat{\mathbf{R}}_{ik}) + \rho_1^{\kappa}(-\hat{\mathbf{z}}_k \cdot \hat{\mathbf{R}}_{ik}) + \rho_2^{\iota}(3[\hat{\mathbf{z}}_i \cdot \hat{\mathbf{R}}_{ik}]^2 - 1)/2 + \rho_2^{\kappa}(3[\hat{\mathbf{z}}_k \cdot \hat{\mathbf{R}}_{ik}]^2 - 1)/2 \quad (2)$$

The geometry for each of the chlorobenzene molecules was optimized at the MP2/6-31G(*d*,*p*) level of theory, within the Gaussian98 software package.[34] The sets of atomic multipoles up to hexadecapole, which comprised the electrostatic model for each molecule, were derived from a distributed multipole analysis (DMA)[35,36] of the wave function using the program GDMA.[37] The DMA effectively describes nonspherical details of the charge distribution, such as lone pairs and π-electron density. The molecular polarizability tensor was also calculated from the charge density by differentiating the electric dipole moment with respect to an applied electric field. The ab initio charge

(20) Wheeler, G. L.; Colson, S. D. *J. Chem. Phys.* **1976**, *65*, 1227.
(21) Munowitz, M. G.; Wheeler, G. L.; Colson, S. D. *Mol. Phys.* **1977**, *34*, 1727.
(22) Wheatley, R. J.; Price, S. L. *Mol. Phys.* **1990**, *71*, 1381.
(23) Tremayne, M.; Grice, L.; Pyatt, J. C.; Seaton, C. C.; Kariuki, B. M.; Tsui, H. H. Y.; Price, S. L.; Cherryman, J. C. *J. Am. Chem. Soc.*, submitted.
(24) Thiéry, M.-M.; Rérat, C. *J. Chem. Phys.* **1998**, *109*, 10940.
(25) Thiéry, M.-M.; Rérat, C. *J. Chem. Phys.* **2003**, *118*, 11100.
(26) Gavezzotti, A. *Acc. Chem. Res.* **1994**, *27*, 309.
(27) Lommerse, J. P. M.; Motherwell, W. D. S.; Ammon, H. L.; Dunitz, J. D.; Gavezzotti, A.; Hofmann, D. W. M.; Leusen, F. J. J.; Mooij, W. T. M.; Price, S. L.; Schweizer, B.; Schmidt, M. U.; van Eijck, B. P.; Verwer, P.; Williams, D. E. *Acta Crystallogr.* **2000**, *B56*, 697.
(28) Beyer, T.; Lewis, T.; Price, S. L. *CrystEngComm* **2001**, *3*, 178.
(29) Motherwell, W. D. S.; Ammon, H. L.; Dunitz, J. D.; Dzyabchenko, A.; Erk, P.; Gavezzotti, A.; Hofmann, D. W. M.; Leusen, F. J. J.; Lommerse, J. P. M.; Mooij, W. T. M.; Price, S. L.; Scheraga, H.; Schweizer, B.; Schmidt, M. U.; van Eijck, B. P.; Verwer, P.; Williams, D. E. *Acta Crystallogr.* **2002**, *B58*, 647.
(30) Gavezzotti, A. *CrystEngComm* **2002**, *4*, 343.
(31) Dunitz, J. D. *Chem. Commun.* **2003**, 545.
(32) Ghelfenstein, M.; Szwarc, H. *Mol. Cryst. Liq. Cryst.* **1971**, *14*, 283.
(33) Dworkin, A.; Figuiere, P.; Ghelfenstein, M.; Szwarc, H. *J. Chem. Thermodyn.* **1976**, *8*, 835.
(34) Frisch, M. J.; Trucks, G. W.; Schlegel, H. B.; Scuseria, G. E.; Robb, M. A.; Chesseman, J. R.; Zakrzewski, V. G.; Montgomery, J. A.; Stratmann, R. E.; Burant, J. C.; Dapprich, S.; Millam, J. M.; Daniels, A. D.; Kudin, K. N.; Strain, M. C.; Farkas, O.; Tomasi, J.; Barone, V.; Cossi, M.; Cammi, R.; Mennucci, B.; Pomelli, C.; Adamo, C.; Clifford, S.; Ochterski, J.; Petersson, G. A.; Ayalla, P. Y.; Cui, Q.; Morokuma, K.; Malick, D. K.; Rabuck, A. D.; Raghavachari, K.; Foresman, J. B.; Cioslowski, J.; Ortiz, J. V.; Stefanov, B. B.; Liu, G.; Liashenko, A.; Piskorz, P.; Komaromi, I.; Gomperts, R.; Martin, R. L.; Fox, D. J.; Keith, T.; Al-Laham, M. A.; Peng, C. Y.; Nanayakkara, A.; Gonzalez, C.; Challacombe, M.; Gill, P. M. W.; Johnson, B. G.; Chen, W.; Wong, M. W.; Andres, J. L.; Head-Gordon, M.; Replogle, E. S.; Pople, J. A. *Gaussian98*, revision A.6 ed.; Gaussian Inc.: Pittsburgh, PA, 1998.
(35) Stone, A. J. *Chem. Phys. Lett.* **1981**, *83*, 233.
(36) Stone, A. J.; Alderton, M. *Mol. Phys.* **1985**, *56*, 1047.
(37) Stone, A. J. *GDMA*, 1.0 ed.; University of Cambridge.

densities for monochlorobenzene and 1,2,3-trichlorobenzene were further used in the derivation of the repulsion model.

Repulsion Models. An atom−atom repulsion model can be derived[23,38−42] by assuming that the repulsion between two molecules is approximately proportional to the overlap of their charge densities,

$$E_{\mathrm{rep}}^{\mathrm{MN}} = K(S_\rho^{\mathrm{MN}})^y \tag{3}$$

where the overlap S_ρ^{MN} is calculated by integrating the (undistorted) monomer charge densities over all spatial coordinates, r,

$$S_\rho^{\mathrm{MN}} = \int \rho_{\mathrm{M}}(r)\rho_{\mathrm{N}}(r)d^3r \tag{4}$$

and the power, y, is typically slightly less than unity.[43] The relationship has been explicitly tested for the repulsion between rare gas atoms and spherical ions,[44] in rare gas dimers,[43] for simple diatomic dimers (Cl_2, N_2, F_2),[45] and for small hydrogen-bonded organic molecules.[38] The advantage of making this approximation is that the total molecular overlap at any orientation can be decomposed into its atom−atom contributions, as implemented in the program GMUL,[46−48] which expresses the molecular charge distribution in terms of atomic contributions. The molecular overlap can be quite cheaply evaluated at a large number of relative orientations of the two molecules, sampling far more relative orientations than would be possible for explicit calculation of either the total intermolecular interaction or its short-range components (i.e., exchange−repulsion, charge−transfer, and penetration). The atom−atom overlaps for every pair of atoms generated in the set of molecular overlap calculations can then be explicitly fitted to give a simple atom−atom model for the overlap, testing whether an anisotropic functional form is appropriate and whether the parameters can be considered transferable. The approximation has been used in developing analytical models for intermolecular interactions in ion−water clusters,[49,50] the solid and liquid phases of molecular chlorine,[45] and the crystal structures of amides,[41] oxalic acid,[39] chlorothalonil ($C_6Cl_4(CN)_2$),[23] cyanuric chloride ($C_3N_3Cl_3$), and other aza-aromatic chlorides.[42]

To be consistent with the atom−atom model, we fitted to a modified version of the power-law relation in eq 3

$$E_{\mathrm{rep}}^{\mathrm{MN}} = K \sum_{i\in\mathrm{M},k\in\mathrm{N}} (S_\rho^{ik})^y \tag{5}$$

and we developed an analytical atom−atom model for the overlap of a pair of monochlorobenzene molecules, of the form

$$S_\rho^{\iota\kappa} = s\exp(-\alpha^{\iota\kappa}[R_{ik} - \rho^{\iota\kappa}(\Omega_{ik})]) \tag{6}$$

where $s = 1$ au of overlap, considering about four hundred different relative orientations, using essentially the methodology described in ref 42. The specific details are given in Supporting Information S1. This was then repeated for pairs of 1,2,3-trichlorobenzene molecules. The individual atom−atom models were compared, and a decision was made on the types of atoms that could be considered transferable, as demonstrated in Supporting Information S2. The final parameters, α, ρ_0, ρ_1, and ρ_2 in eqs 2 and 6, were then fitted to the total overlap data for each atomic type from both molecules. An isotropic model, with ρ independent of orientation, was also fitted for comparison.

The proportionality constant K and the power y were obtained by fitting the overlap to the short-range interaction energies of the monochlorobenzene dimer, calculated at 30 different geometries, chosen to sample a range of overlaps and orientations for each pair of atom types. IMPT energies, using a 6-31G(d) basis set, were calculated within the program CADPAC[51] to provide the exchange, repulsion, and charge-transfer contributions to the intermolecular interaction. The penetration energy was calculated as the difference between the IMPT electrostatic energy and the electrostatic interaction between monomers calculated from the DMA electrostatic model,

$$E_{\mathrm{penetration}} = E_{\mathrm{electrostatic}}^{\mathrm{IMPT}} - E_{\mathrm{electrostatic}}^{\mathrm{DMA}} \tag{7}$$

using the program ORIENT.[52]

The exchange−repulsion, charge−transfer, and penetration contributions are all expected to decay exponentially with interatomic separation, so the parameters, K and y, were fitted to the sum of these energies, minimizing squared deviations between IMPT and model energies. Other forms of fitting to the IMPT energies were investigated, as well as optimizing K empirically to reproduce the crystal structures. However, as shown in Supporting Information S5, the best-justified fit to the IMPT energies also seemed most satisfactory in reproducing the crystal structures and properties.

Dispersion Models. Although methods are being developed,[53] it is not yet possible to routinely derive an accurate anisotropic atom−atom model of dispersion directly from the charge distribution of an organic molecule. Hence, we assumed an effective isotropic C_6 atom−atom dispersion model, using the Slater−Kirkwood relationship of dispersion to atomic polarizabilities.

$$C_6^{\iota\kappa} = \frac{3}{2}\frac{\alpha_\iota\alpha_\kappa}{(\alpha_\iota/N_\iota^{\mathrm{eff}})^{1/2} + (\alpha_\kappa/N_\kappa^{\mathrm{eff}})^{1/2}} \tag{8}$$

We considered several choices for the atomic polarizabilities, α_ι, and effective number of electrons, N^{eff}. The dispersion coefficients in the final model were calculated with $N^{\mathrm{eff}} = N_{\mathrm{v}}$, the number of valence electrons of atom type ι (i.e., $N_{\mathrm{Cl}}^{\mathrm{eff}} = 7$, $N_{\mathrm{C}}^{\mathrm{eff}} = 4$, $N_{\mathrm{H}}^{\mathrm{eff}} = 1$), and ab initio derived atomic polarizabilities, using a scaling factor which could be justified as allowing for their underestimation in the ab initio calculations. These atomic polarizabilities, α_ι, were fitted to MP2/6-31G(d,p) calculated molecular polarizability tensors of the chlorobenzenes so as to minimize the root-mean-squared deviation between the sum of atomic and mean molecular polarizabilities, $\bar{\alpha} = (\alpha_{xx} + \alpha_{yy} + \alpha_{zz})/3$. The other possibilities that we considered were the smaller N^{eff} values proposed by Halgren[54] ($N_{\mathrm{Cl}}^{\mathrm{eff}} = 5.10$, $N_{\mathrm{C}}^{\mathrm{eff}} = 2.49$, and $N_{\mathrm{H}}^{\mathrm{eff}} = 0.80$) on the basis of modeling the actual induced-dipole, induced-dipole C_6, rather than total effective dispersion, and Miller's tabulation[55] of empirically derived atomic polarizabilities. Testing of the possible combinations of α values and N^{eff} is described in Supporting Information S3 and S5.

Testing the Model Potentials

Model potentials were tested for their ability to reproduce the known crystal structures for 10 of the chlorobenzenes: monochlorobenzene,[56] *ortho*-,[57] *meta*-,[57] and *para*-dichlorobenzene (all three polymorphs),[20] 1,2,3-[58] and 1,3,5-trichloroben-

(38) Nobeli, I.; Price, S. L.; Wheatley, R. J. *Mol. Phys.* **1998**, *95*, 523.
(39) Nobeli, I.; Price, S. L. *J. Phys. Chem. A.* **1999**, *103*, 6448.
(40) Tsui, H. H. Y.; Price, S. L. *CrystEngComm* **1999**, *1*, 24.
(41) Mitchell, J. B. O.; Price, S. L. *J. Phys. Chem. A.* **2000**, *104*, 10958.
(42) Mitchell, J. B. O.; Price, S. L.; Leslie, M.; Buttar, D.; Roberts, R. J. *J. Phys. Chem. A* **2001**, *105*, 9961.
(43) Kim, Y. S.; Kim, S. K.; Lee, W. D. *Chem. Phys. Lett.* **1981**, *80*, 574.
(44) Kita, S.; Noda, K.; Inouye, H. *J. Chem. Phys.* **1976**, *64*, 3446.
(45) Wheatley, R. J.; Price, S. L. *Mol. Phys.* **1990**, *69*, 507.
(46) Wheatley, R. J. *Mol. Phys.* **1993**, *79*, 597.
(47) Wheatley, R. J.; Mitchell, J. B. O. *J. Comput. Chem.* **1994**, *15*, 1187.
(48) Wheatley, R. J. *GMUL3s*; University of Nottingham: 1996.
(49) Wheatley, R. J.; Hutson, J. M. *Mol. Phys.* **1995**, *84*, 879.
(50) Wheatley, R. J. *Mol. Phys.* **1996**, *87*, 1083.
(51) Amos, R. D. (with contributions from I. L. Alberts, J. S. A., S. M. Colwell, N. C. Handy, D. Jayatilaka, P. J. Knowles, R. Kobayashi, N. Koga, K. E. Laidig, P. E. Maslen, C. W. Murray, J. E. Rice, J. Sanz, E. D. Simandiras, A. J. Stone, and M.-D. Su) *CADPAC*, 6.0 ed.: University of Cambridge: 1995.
(52) Stone, A. J.; Dullweber, A.; Hodges, M. P.; Popelier, P. L. A.; Wales, D. J.; *ORIENT*, 3.2 ed.; University of Cambridge: 1996.
(53) Hodges, M. P.; Stone, A. J. *Mol. Phys.* **2000**, *98*, 275.
(54) Halgren, T. A. *J. Am. Chem. Soc.* **1992**, *114*, 7827.
(55) Miller, K. J. *J. Am. Chem. Soc.* **1990**, *112*, 8533.

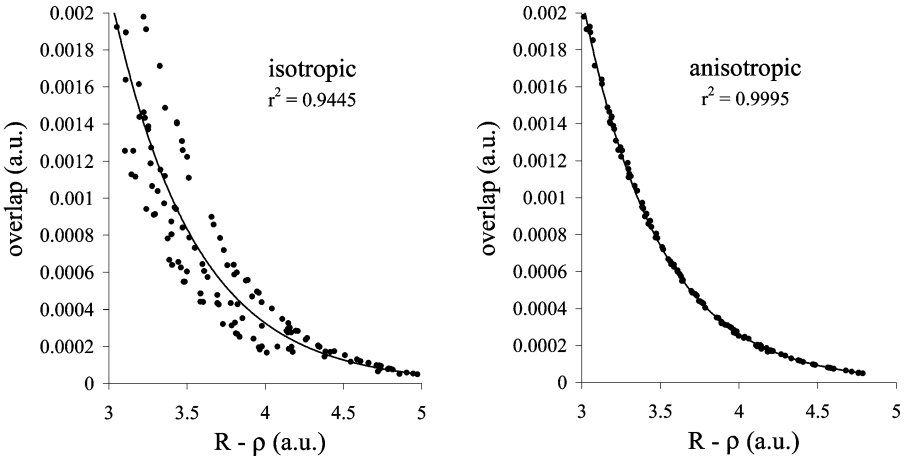

Figure 2. Fitting to the overlap between chlorine atoms in monochlorobenzene dimers using the model in eq 6, with an isotropic radial parameter, ρ, (left) and the anisotropic model in eq 2 (right). Similar results were obtained for 1,2,3-trichlorobenzene.

zene,[59] 1,2,3,5-[60] and 1,2,4,5-tetrachlorobenzene,[61] pentachlorobenzene,[62] and hexachlorobenzene.[63] The lattice energy minimum, starting from the experimental crystal structure and using a rigid ab initio optimized molecular geometry, was found using the program DMAREL.[64,65] Repulsion−dispersion contributions to the lattice energy were summed to 15 Å, charge−charge, charge−dipole, and dipole−dipole electrostatic terms using Ewald summation and higher order electrostatic contributions (up to R^{-5}) to a 15 Å cutoff between molecular centers of mass.

Elastic constants and $\mathbf{k} = 0$ intermolecular phonon frequencies were calculated from the second derivatives of the lattice energy.[66,67] For comparison with low-temperature spectra, the vibrational modes were calculated at the minimum in lattice energy, while comparisons were made with higher temperature spectra through the quasi-harmonic approximation, fixing the lattice constants at observed values nearest the temperature of the spectrum. Thermodynamical calculations used the Einstein approximation of no dispersion for optic modes and the Debye model for the acoustic modes, estimating the cutoff frequency from calculated wave velocities.

For the crystal structure prediction of *p*-dichlorobenzene, densely packed hypothetical structures were generated using the program MOLPAK[68] in 41 common coordination geometries, belonging to the space groups $P1$, $P\bar{1}$, $P2_1$, $P2_1/c$, $P2_12_12$, $P2_12_12_1$, $Pna2_1$, $Pca2_1$, $Pbca$, $Pbcn$, $C2/c$, Cc, and $C2$, with $^1/_2$ or 1 molecule in the asymmetric unit (Z'). Nearly 95% of known organic molecular crystals are covered by these space groups,[69] and many of the less common, higher symmetries can be located in searches of these space groups. We are, therefore, unlikely to miss many low energy structures in the search.

Approximately 1800 trial structures were then lattice energy minimized in the program DMAREL. The initial MOLPAK symmetry was used in the minimizations but relaxed to a subgroup if instabilities in the elastic stiffness matrix or phonon frequencies were found. We used the attachment energy model[70] to estimate the relative growth rates of all the crystal faces of the lowest energy crystal structures, using the Cerius2 software[71] and the pcff force field[72] with charges fitted to the ab initio molecular electrostatic potential. The volume of each growth morphology was numerically integrated using our own software to obtain total relative growth rates.

Results

Investigation of Transferability and Anisotropy in the Atom−Atom Overlap. The atom−atom overlaps for monochlorobenzene and 1,2,3-trichlorobenzene (Supporting Information S2) show sufficient similarities to define transferable atomic types. There was very little variation in the hydrogen atom parameters and there were only minor differences between the three distinct chlorine atoms. However, variations among the carbon atoms are quite substantial, and the parameters reflect that carbons bonded to chlorine, C_{Cl}, have a charge density that falls off more rapidly with distance (larger α) than carbons bonded to hydrogen, C_H. There is variability among the other carbon atoms, due to resonance and inductive effects of atoms that are not directly bonded. For example, the radial behavior of the *meta* carbon atom is harder than the other (*ortho* and *para*) non-chlorinated carbon atoms in monochlorobenzene, and in 1,2,3-trichlorobenzene, the carbon that is in a *meta* position to two chlorine atoms is harder still. Despite this type of variation, which shows the limitations of a transferable model, it seemed worthwhile proceeding on the basis that all H atoms and all Cl atoms are of the same type and that there are two distinct types of carbon, C_{Cl} and C_H.

Analysis of the Cl···Cl overlaps clearly showed that they did not solely depend on the separation of the atoms and that the atoms were anisotropic. An excellent fit could be obtained (Figure 2) when the variation in the repulsion with the angle of

(56) Andre, D.; Fourme, R.; Renaud, M. *Acta Crystallogr.* **1971**, *B27*, 2371.
(57) Boese, R.; Kirchner, M. T.; Dunitz, J. D.; Filippini, G.; Gavezzotti, A. *Helv. Chim. Acta* **2001**, *84*, 1561.
(58) Groke, D.; Heger, G.; Schweiss, B. P.; Weiss, A. *Z. Naturforsch., A: Phys. Sci.* **1994**, *49*, 599.
(59) Milledge, H. J.; Pant, L. M. *Acta Crystallogr.* **1960**, *13*, 285.
(60) Marsh, P.; Williams, D. E. *Acta Crystallogr.* **1981**, *B37*, 279.
(61) Anderson, D. G.; Blake, A. J.; Blom, R.; Cradock, S.; Rankin, D. W. H. *Acta Chem. Scand.* **1991**, *45*, 158.
(62) Marsh, P.; Williams, D. E. *Acta Crystallogr.* **1981**, *B37*, 705.
(63) Strel'tsova, I. N.; Struchkov, Y. T. *Zh. Strukt. Khim.* **1961**, *2*, 312.
(64) Willock, D. J.; Price, S. L.; Leslie, M.; Catlow, C. R. A. *J. Comput. Chem.* **1995**, *16*, 628.
(65) Price, S. L.; Willock, D. J.; Leslie, M.; Day, G. M. *DMAREL*, 3rd ed.; CCP5 CCLRC: Daresbury, 2001.
(66) Day, G. M.; Price, S. L.; Leslie, M. *Cryst. Growth Des.* **2000**, *1*, 13.
(67) Day, G. M.; Price, S. L.; Leslie, M. L. *J. Phys. Chem. B* **2003**, *107*, 10919.
(68) Holden, J. R.; Du, Z. Y.; Ammon, H. L. *J. Comput. Chem.* **1993**, *14*, 422.
(69) Brock, C. P.; Dunitz, J. D. *Chem. Mater.* **1994**, *6*, 1118.
(70) Hartman, P.; Perdok, W. *Acta Crystallogr.* **1955**, *8*, 49.
(71) *Cerius2*, version 4.6; Molecular Simulations Inc.: San Diego, CA, 1997.
(72) Sun, H. *J. Comput. Chem.* **1994**, *15*, 752.

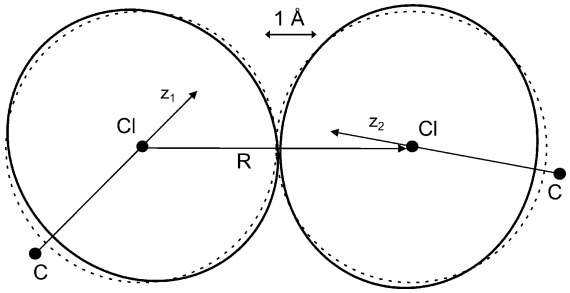

Figure 3. Repulsive wall around the chlorine atoms, showing the differences between the anisotropic model for repulsion (solid contours) and the corresponding isotropic model (dashed contours). To display the repulsion as an atomic property, we have factorized the overlap between atoms as $S_\rho^{ClCl} = W_1^{Cl}W_2^{Cl}$, where $W_1^{Cl} = s\exp(-\alpha^\iota[R_{ClCl} - \{\rho_0^{ClCl}/2 + \rho_1^{Cl}(\hat{\mathbf{z}}_{Cl1}\cdot\hat{\mathbf{R}}_{ClCl}) + \rho_2^{Cl}(3[\hat{\mathbf{z}}_{Cl1}\cdot\hat{\mathbf{R}}_{ClCl}]^2 - 1)/2\}])$ and plotted contours of constant W_1^{Cl} at a value chosen to represent the repulsion at typical van der Waals contact distances.

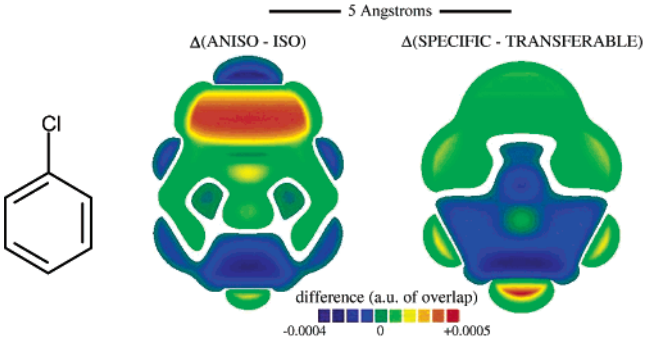

Figure 4. Errors in modeling the overlap by either an isotropic or transferable atom−atom model. Assuming that contributions are split between atoms as in Figure 3, the molecular surface for monochlorobenzene was calculated from the molecule-specific anisotropic atom−atom model, and this surface is colored by the difference in overlap between anisotropic and isotropic, $\Delta = (S_{\rho,aniso} - S_{\rho,iso})$, (left) and specific and transferable, $\Delta = (S_{\rho,aniso,specific} - S_{\rho,aniso,transferable})$, (right) models.

the intermolecular contact was modeled by the simple form of eq 2. Over 99% of the deviation between predicted and accurate overlaps in the isotropic model is removed by introducing this predominantly quadrupolar anisotropy which describes a polar flattening along the C−Cl bond, with a broadening in the directions of lone pair density. The extent of this anisotropy is illustrated in Figure 3. While the anisotropy is not dramatic, it is sufficient to lead to variations in contact distances of order of 0.1−0.2 Å, corresponding to the observed anisotropy in van der Waals contacts.[7]

The carbon atoms bonded to chlorine were also found to have a marked anisotropy, which contributes to the overall broadening around the C−Cl moiety, while the polar nature of the bond also pulls electron density away from the center of the aromatic ring. There was also a dipolar distortion of the *para* carbon atom apparent in both molecules, shifting the center of overlap distribution away from the nucleus, in the direction of the molecular dipole moment. This latter effect could not be maintained in a transferable scheme which does not distinguish between different C_H carbon atoms and so produces the largest errors from assuming transferability (Figure 4). Although the anisotropic terms describing hydrogen−hydrogen interactions are much less important than those for the other atoms, the small negative ρ_1^H parameters shift the center of the exponential distribution into the C−H bond, away from the nucleus and toward the true center of charge density. Thus, the introduction

Table 1. Final, Transferable Anisotropic Atom−Atom Model Potential[a]

atom types		$A^{\iota\kappa}$,	$B^{\iota\kappa}$,	$C_6^{\iota\kappa}$,	ρ_1^ι,	ρ_1^κ,	ρ_2^ι,	ρ_2^κ,
ι	κ	kJ/mol	Å^{-1}	Å^6 kJ/mol	Å	Å	Å	Å
Cl	Cl	569746	3.3427	8366.9	+0.0156	+0.0156	−0.0939	−0.0939
C_{Cl}	C_{Cl}	28957	3.2131	2146.4	−0.2054	−0.2054	−0.3109	−0.3109
C_H	C_H	107333	3.1936	2146.4	−0.0026	−0.0026	+0.0419	+0.0419
H	H	2220	3.2575	200.0	−0.0449	−0.0449	+0.0036	+0.0036
Cl	C_{Cl}	277307	3.5474	4234.3	+0.0156	−0.2054	−0.0939	−0.3109
Cl	C_H	219400	3.2465	4234.3	+0.0156	−0.0026	−0.0939	+0.0419
Cl	H	30829	3.2597	1293.1	+0.0156	−0.0449	−0.0939	+0.0036
C_{Cl}	C_H	61374	3.2443	2146.4	−0.2054	−0.0026	−0.3109	+0.0419
C_{Cl}	H	11254	3.3709	653.7	−0.2054	−0.0449	−0.3109	+0.0036
C_H	H	16950	3.2654	653.7	−0.0026	−0.0449	+0.0419	+0.0036

[a] C_{Cl} is a carbon bonded to chlorine; C_H is a carbon bonded to hydrogen. Atomic *z*-axes are defined along the bonds pointing out from the aromatic ring (Figure 1). The isotropic term in ρ has been converted into a pre-exponential factor, $A = \exp(-y\alpha\rho_0)$, for easier comparison with the more common form of the *exp*-6 model potential, and $B = y\alpha$ incorporates the fitted value of $y = 0.8331$.

of anisotropy considerably improves the accuracy of the model for the overlaps, with the major improvements being around the chlorine atoms and above the *para* carbon atoms. The ratio of root-mean-square errors in fitting to the exact overlaps with the isotropic and anisotropic models is 6.7. The errors introduced by using a transferable model, fitted to the overlap data of both molecules, rather than a specific model for that molecule, are less significant; the ratio of root-mean-square errors in the molecule−molecule overlaps is 1.2.

Converting the anisotropic atom−atom model for the overlap into a repulsion model required least-squares fitting to the sum of the exchange, repulsion, charge-transfer, and penetration energies at 30 dimer orientations. The results (Supporting Information S4) showed that the transferable model for the overlap could be fitted to the IMPT points almost as well as the original total overlaps. Hence the loss in accuracy through the assumption of transferability and the overlap fitting procedure was not significant compared with the errors in the initial assumption of the overlap model (eq 3).

The derivation of a set of atomic polarizabilities from the ab initio calculated mean molecular polarizabilities was successful, as all 10 molecular polarizabilities were reproduced to within 1.1%. Testing various dispersion models in conjunction with the fixed repulsion and electrostatic model (Supporting Information S5) revealed that the ratio of Cl to C and H dispersion of the ab initio derived atomic polarizabilities seemed more appropriate than Miller's more generic empirically fitted values. However, the dispersion contribution was too weak, partly because the calculated molecular polarizabilities are approximately 20% lower than experimental values for mono- and 1,2,3-dichlorobenzene,[73] an underestimate typical of ab initio polarizability calculations.[74] This is in line with the atomic polarizabilities, on average, being similarly smaller in magnitude than Miller's empirically fitted values.[55] Treating a scaling of the atomic polarizabilities in the Slater−Kirkwod formula as an empirical factor and roughly optimizing this to the 100 K *p*-dichlorobenzene crystal structures produced a scale factor of 1.29, which reasonably accounts for the underestimate in the ab initio determination. The use of low-temperature crystal structures in this step should minimize the thermal effects

(73) Landolt-Bornstein, Ed. *Atom und Molekularphysik*; Springer-Verlag: West Berlin, 1951; Vol. 1, Part 3, pp 511−513.
(74) Ewig, C. S.; Waldman, M.; Maple, J. R. *J. Phys. Chem.* **2002**, *A106*, 326.

Table 2. Reproduction of the Crystal Structures of the Chlorobenzene Molecules by Lattice Energy Minimization with the Nonempirical Model Potential

Deviations in Lattice Parameters, Volumes, and the Structural Drift Factor

crystal	space group	*a* (Å)	*b* (Å)	*c* (Å)	β (deg)	ΔV (%)	*F*
C_6H_5Cl	*Pbcn*	13.53	10.98	7.27	90	−2.87	11.53
T = 120 K[56]		(+0.10%)	(−2.41%)	(−0.56%)			
o-$C_6H_4Cl_2$	$P2_1/n$	3.89	10.46	14.98	95.24	−4.60	17.39
T = 223 K[57]		(−1.50%)	(−1.57%)	(−1.93%)	(−1.82%)		
m-$C_6H_4Cl_2$	$P2_1/c$	3.87	12.38	25.62	91.84	−4.55	17.05
T = 220 K[57]	($Z' = 2$)	(−1.29%)	(−1.63%)	(−1.77%)	(−1.11%)		
α *p*-$C_6H_4Cl_2$	$P2_1/a$	14.64	5.62	3.97	113.87	−2.58	12.78
T = 100 K[20]	($Z' = {}^1/_2$)	(−0.16%)	(−2.05%)	(+1.16%)	(+1.88%)		
β *p*-$C_6H_4Cl_2$	$P\bar{1}$	7.26	5.86	3.87	α = 91.82 (+0.76%)	−2.30	6.16
T = 100 K[20]	($Z' = {}^1/_2$)	(−0.53%)	(−0.28%)	(−0.21%)	β = 114.05 (+1.33%)		
					γ = 93.24 (+0.88%)		
γ *p*-$C_6H_4Cl_2$	$P2_1/c$	8.16	6.19	7.39	126.48	−1.76	49.38
T = 100 K[20]	($Z' = {}^1/_2$)	(−5.38%)	(+2.80%)	(−0.36%)	(−0.81%)		
1,2,3-$C_6H_3Cl_3$	$P2_1/c$	12.52	8.11	14.90	114.66	−0.26	1.91
T = 158 K[58]	($Z' = 2$)	(+0.72%)	(−0.44%)	(−0.25%)	(+0.32%)		
1,3,5-$C_6H_3Cl_3$	$P2_12_12_1$	13.75	12.95	3.88	90	−3.81	9.71
T = 90 K[59]		(−1.32%)	(−1.81%)	(−0.72%)			
1,2,3,5-$C_6H_2Cl_4$	$P2_1/c$	3.81	23.53	17.30	96.16	−3.04	24.07
room temp[60]	($Z' = 2$)	(−1.17%)	(−1.98%)	(+0.41%)	(+2.17%)		
1,2,4,5-$C_6H_2Cl_4$	$P2_1/a$	3.80	10.62	9.50	100.62	+0.19	9.14
T = 173 K[61]	($Z' = {}^1/_2$)	(+0.19%)	(+0.98%)	(−0.69%)	(+0.90%)		
C_6HCl_5	$Pca2_1$	16.74	3.81	13.36	90	−1.04	4.21
room temp[60]		(−0.36%)	(−1.27%)	(+0.59%)			
C_6Cl_6	$P2_1/c$	8.08	3.77	16.81	117.33	−2.10	8.62
room temp[63]	($Z' = {}^1/_2$)	(−0.05%)	(−2.67%)	(+0.94%)	(+0.29%)		

overall	overall RMS error for the lattice constants, *a*,*b*,*c* (%)	mean ΔV (%)	$\sum F$
final model (Table 1)	1.57	−2.39	171.95
HW + DMA[a]	2.25	+0.51	477.93
HW + point charges[a]	2.47	+1.27	572.49

Deviations in Cl···Cl Contact Distances and Angles and Comparison of Calculated and Observed Enthalpies of Sublimation

crystal	mean $\Delta R_{Cl\cdots Cl}$[b] (Å)	mean $\Delta\theta_{C-Cl\cdots Cl}$[b] (deg)	$4RT - (\Phi_{latt} + E_{crystal}^{inter,vib})$[c] (kJ/mol)	$\Delta H°_{sub}$ (obsd) (kJ/mol)
C_6H_5Cl	0.08	1.9	56.46 (208 K)	
o-$C_6H_4Cl_2$	0.09	1.5	65.64 (223 K)	
m-$C_6H_4Cl_2$	0.02	1.4	64.66 (220 K)	
α *p*-$C_6H_4Cl_2$	0.08	0.6	66.47 (298 K)	64.75 ± 0.15[76]
β *p*-$C_6H_4Cl_2$	0.01	1.4	66.59 (298 K)	64.57 ± 0.15[76]
γ *p*-$C_6H_4Cl_2$	0.02	4.5	66.97[d] (298 K)	65.98 ± 0.15[76]
123-$C_6H_3Cl_3$	0.06	0.8	73.21 (298 K)	75.1 ± 0.75[77]
135-$C_6H_3Cl_3$	0.04	1.7	72.22 (298 K)	70.74 ± 0.05[78]
1235-$C_6H_2Cl_4$	0.05	2.0	79.83 (298 K)	79.56 ± 0.32[79]
1245-$C_6H_2Cl_4$	0.05	1.2	82.62 (298 K)	82.10 ± 0.07[78]
C_6HCl_5	0.02	1.5	87.35 (298 K)	87.12 ± 0.36[79]
C_6Cl_6	0.03	0.8	95.47 (298 K)	90.50 ± 0.19[79]

	overall mean $\Delta R_{Cl\cdots Cl}$	overall mean $\Delta\theta_{C-Cl\cdots Cl}$	mean absolute difference (kJ/mol)
final model	0.04	1.5	1.56
HW + DMA	0.07	3.3	1.28
HW + point charges	0.10	3.7	1.65

[a] For comparison, averages are presented for the empirical model of Hsu and Williams,[18] with DMA and (electrostatic potential fitted) ESP point charge electrostatic models. [b] Averaged over all Cl···Cl contacts shorter than the sum of van der Waals radii + 0.2 Å (3.8 Å). [c] The calculated sublimation enthalpy, where Φ_{latt} is the lattice energy calculated using the finite temperature unit cell parameters, $E_{crystal}^{inter,vib}$ is the lattice mode contribution to the vibrational zero-point energy and integral over the heat capacity, C_P, and the factor $4RT$ arises from assuming an ideal gas for the gas-phase enthalpy. [d] Lattice energy calculated at 260 K structure and corrected by 0.5 kJ/mol for the difference to 298 K.

absorbed into the potential. This was the single parameter used in developing the final model potential that was not derived from the calculated wave functions. The set of final parameters is given in Table 1.

Testing the Model

Table 2 shows that the final potential reproduces all the crystal structures acceptably, within the accuracy that can be expected in comparing lattice energy minima with finite temperature crystal structures. Almost all the crystal volumes decrease when the lattice energy is minimized, consistent with the lattice energy minimum corresponding roughly to $T = 0$ K. All cell lengths are reproduced slightly better than those with the empirically fitted isotropic repulsion-dispersion model of Hsu and Williams,[18] combined with either atomic charges or a DMA electrostatic model (Supporting Information S5 provides details). However, the major improvement is in the molecular positions and orientations within the lattice, which is reflected in the structural drift factor, *F*.[75]

Using the isotropic empirical model, the molecular rotations are unacceptable for the more heavily chlorinated molecules; 1,2,4,5-tetrachlorobenzene, pentachlorobenzene, and hexachlo-

Table 3. **k** = 0 Intermolecular Harmonic Phonon Spectra Calculated from the Final Model Potential at the Fully Relaxed Structures (Room Temperature Quasi-harmonic Calculations in Italics, and Experimental Values in Parentheses; All in cm^{-1})

	low-temperature spectra				room-temperature spectra		
	α *p*-$C_6H_4Cl_2$ $T = 1.2$ K[80]	β *p*-$C_6H_4Cl_2$[a] $T = 1.2$ K[80]	γ *p*-$C_6H_4Cl_2$ $T = 1.2$ K[80]	C_6Cl_6 $T = 77$ K[81]	1,2,4,5-$C_6H_2Cl_4$ room temp[82,83]		1,3,5-$C_6H_3Cl_3$[b] room temp[84,85]
A_g	108.5 (109)	96.2 (103)	111.1 (143)	56.2 (64)	64.2 *63.8* (57.5)	A_1	65.3 *57.3* (58)
	67.0 (66)	62.4 (65)	65.0 (67)	42.8 (50)	51.6 *51.4* (45)		26.8 *23.9* (23)
	53.2 (NA)[c]	56.6 (56)	52.5 (52)	21.2 (26)	38.7 *34.5* (35.5)		
B_g	117.5 (117)		114.1 (133)	53.5 (60)	53.3 *57.7* (NA)	B_1	69.1 *59.8* (62.5)
	57.0 (59)		81.2 (86)	37.8 (45)	50.8 *45.2* (49)		39.3 *34.3* (34.5)
	29.5 (33)		55.2 (76)	23.7 (31)	27.4 *24.6* (20)	B_2	63.2 *55.5* (56.5)
A_u	66.0 (67[d])		102.4 (NA)	52.1 (NA)	69.7 *66.6* (NA)		25.9 *22.0* (22.5)
	45.8 (46[d])		44.6 (NA)	41.1 (NA)	47.9 *35.5* (NA)	B_3	69.2 *60.3* (58)
B_u	35.8 (27[d])		44.8 (NA)	21.5 (NA)	67.3 *56.8* (NA)		36.0 *31.1* (30)

[a] β *p*-dichlorobenzene has only 3 spectra lines at **k** = 0. [b] There are 21 optic lattice modes for 1,3,5-trichlorobenzene. We give the highest and lowest of each symmetry type here, and the complete set is given in the Supporting Information S6. [c] NA = not available. [d] Extrapolated to $T = 0$ K from Wincke's data at 80 K and 300 K.[86]

robenzene all rotate by more than 10° away from their observed orientations with either electrostatic model. In contrast, the anisotropic model reproduces the molecular orientations and Cl···Cl closest contacts well, reproducing the range from 3.39 Å in β-dichlorobenzene to 3.8 Å in γ-dichlorobenzene to within 0.1 Å.

The predicted heats of sublimation (calculated from the lattice energies, phonon frequencies, and an ideal gas model) are close to the observed values and, certainly, given the experimental errors and uncertainties in this relationship, give no cause for concern about the quality of the potential. This is noteworthy as energetic data were not used in the derivation of the potential, in contrast with the empirically fitted HW model.

As well as the structures and sublimation enthalpies, we evaluate the model on its ability to reproduce phonon spectra and thermodynamic and mechanical properties of the chlorobenzenes. Calculated frequencies have been classified by the irreducible representations of the vibrations (A_g, B_u, etc.) in the point groups C_i (β *p*-dichlorobenzene), C_{2h} (α and γ *p*-dichlorobenzene, 1,2,4,5-tetrachlorobenzene, and hexachlorobenzene), and D_2 (1,3,5-trichlorobenzene). In most cases, these show very good agreement with the observed low frequency Raman and IR spectra (Table 3). The harmonic calculations correspond closely to $T = 0$ K, so show best agreement with the low energy spectra of *p*-dichlorobenzene and hexachlorobenzene. The largest errors are in the highest frequency modes of the γ *p*-dichlorobenzene spectrum, where coupling with intramolecular modes might be important, given the observed distortion of the molecule.[20] For comparison with the room-temperature spectra of 1,3,5-trichlorobenzene and 1,2,4,5-tetrachlorobenzene, we also calculated quasi-harmonic frequencies by fixing the unit cell parameters at their observed values near room temperature. These quasi-harmonic calculations are in much better agreement with the observed spectra than the harmonic results.

Heat capacities are one of the most directly measurable of thermodynamic quantities and have been measured for several of the chlorobenzenes.[33,87−89] We tested the model potential against these observations, calculating the heat capacity from quasi-harmonic phonon calculations at all temperatures where there are lattice constants available (Figure 5). For these calculations, we used the Einstein approximation for the optic frequencies (ω_E) and the Debye model for dispersion of the acoustic modes, with the Debye cutoff frequency (ω_D) calculated from the elastic constant tensor, sinusoidally extrapolating the slope of the acoustic modes (i.e., the sound velocity) to the Brillouin zone boundary in several high-symmetry directions.

$$C_P = k_B \sum_{i>3} \left(\frac{\hbar\omega_E^i}{k_B T}\right)^2 \exp\left(\frac{\hbar\omega_E^i}{k_B T}\right)\left[\exp\left(\frac{\hbar\omega_E^i}{k_B T}\right) - 1\right]^{-2} + 12 k_B D\left(\frac{\hbar\omega_D}{k_B T}\right) - \frac{9\hbar\omega_D}{T}\left[\exp\left(\frac{\hbar\omega_D}{k_B T}\right) - 1\right]^{-1} + TV\beta^2/K_T \quad (9)$$

The first three terms in eq 9 give the constant volume heat capacity, which we corrected (the final term in eq 9) to C_P, using the observed thermal expansion coefficient, β, and isothermal compressibility, K_T, from the calculated elastic compliance tensor. The agreement with experiment is excellent for the *p*-dichlorobenzene polymorphs over the temperature range of approximately 20 to 340 K for the α and γ forms (Figure 5). Our calculated 300 K heat capacity of the β form, $C_P = 149.7$ J/mol K, is in good agreement with the observed 310 K value of 153.4 J/mol K.[33] Errors for 1,2,4,5-tetrachloro- and hexachlorobenzene are slightly higher but generally less than 5−6%.[90]

Finally, the elastic constants of 1,3,5-trichlorobenzene are available (Table 4), and as we found for a series of organic

(75) $$F = \left(\frac{\Delta\theta}{2}\right)^2 + (10\Delta x)^2 + \sum_{\tau=a,b,c}\left(100\frac{\Delta\tau}{\tau}\right)^2 + \sum_{\chi=\alpha,\beta,\gamma}(\Delta\chi)^2$$

where $\Delta\theta$ are molecular rotations, Δx are molecular translations, $\Delta\tau$ and $\Delta\chi$ are deviations in unit cell lengths and angles. See: Williams, D. E. *PCK83, QCPE Program 548. Quantum Chemistry Program Exchange*; Chemistry Department, Indiana University: Bloomington, IN, 1983.

(76) Oonk, H. A. J.; van Genderen, A. C. G.; Blok, J. G.; van der Linde, P. R. *Phys. Chem. Chem. Phys.* **2000**, *2*, 5614.
(77) Ye, H. K.; Gu, J. K.; Fu, R. H. *Wuli Huaxue Xuebao* **1989**, *5*, 487.
(78) Blok, J. G.; van Genderen, A. C. G.; van der Linde, P. R.; Oonk, H. A. J. *J. Chem. Thermodyn.* **2001**, *33*, 1097.
(79) Sabbah, R.; An, X. W. *Thermochim. Acta* **1991**, *179*, 81.
(80) Jongelenis, A. P. J. M.; van der Berg, T. H. M.; Schmidt, J.; van der Avoird, A. *J. Phys.: Condens. Matter* **1989**, *1*, 5051.
(81) Bates, J. B.; Thomas, D. M.; Bandy, A.; Lippincott, E. R. *Spectrochim. Acta* **1971**, *27A*, 637.
(82) D′Alessio, E. A.; Bonadeo, H. *Chem. Phys. Lett.* **1973**, *22*, 559.
(83) White, K. M.; Eckhardt, C. J. *J. Chem. Phys.* **1989**, *90*, 4709.
(84) Muller, D. E.; Inoue, T.; Larkin, R. H.; Stidham, H. D. *Spectrochim. Acta* **1969**, *27A*, 405.
(85) Swanson, D.; Brunel, L.-C.; Dows, D. A. *J. Chem. Phys.* **1975**, *63*, 3863.
(86) Wincke, B.; Hadni, A.; Gerbaux, X. *Le Journal de Physique* **1970**, *31*, 893.
(87) Andrews, D. H.; Haworth, E. *J. Am. Chem. Soc.* **1928**, *50*, 2998.
(88) Hildenbrand, D. L.; Kramer, W. R.; Stull, D. R. *J. Phys. Chem.* **1958**, *62*, 958.
(89) Dworkin, A.; Figuiere, P.; Ghelfenstein, M.; Szwarc, H. Thermodynamic properties of the three solid phases of *p*-dichlorobenzene, Quatrieme Conference International de Thermodynamique Chimique; 1975; Vol. II Thermophysique.

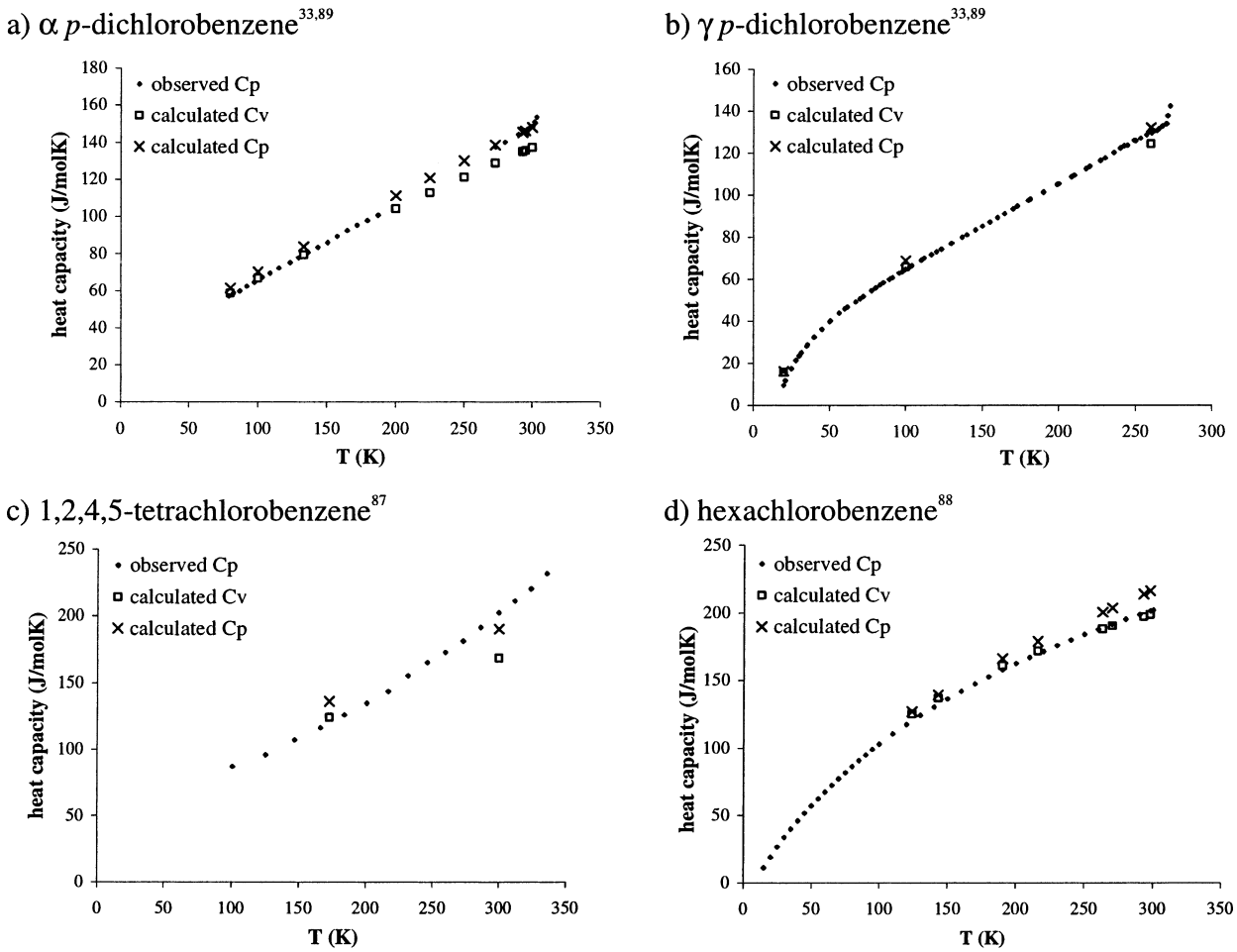

Figure 5. Calculated (C_V and C_P) and observed (C_P) heat capacity curves for four chlorobenzene crystals.

Table 4. Calculated and Observed[85] Elastic Stiffness Constants of 1,3,5-Trichlorobenzene

	observed (room temp) (GPa)	calculated (harmonic, $T = 0$ K) (GPa)
C_{11}	8.03 ± 0.11	11.00
C_{22}	10.98 ± 0.25	16.74
C_{33}	7.89 ± 0.31	12.25
C_{44}	3.49 ± 0.36	1.57
C_{55}	3.75 ± 0.35	4.74
C_{66}	3.38 ± 0.38	6.41
C_{12}	4.47 ± 0.80	6.56
C_{13}	3.85 ± 0.69	9.07
C_{23}	3.88 ± 0.78	4.06

molecular crystals,[66] the calculated values are overestimated, mainly due to the significant temperature dependence of these quantities. Despite the general overestimate, the anisotropy of the uniaxial stiffness constants is reproduced quite well.

The final test of our model potential is the lattice energy search for the polymorphs of *p*-dichlorobenzene. The crystal structure search produced many low energy structures, almost 70 within 5 kJ/mol of the most stable structure (Figure 6), well within the energy range for possible polymorphs. The three known forms were found as the second, third, and fourth most stable by lattice energy, and the low energy structures all share similar packing of the molecules (Figure 7). The lowest energy structure (denoted FC26) is very closely related to the known α and β forms; the lattice constants show a cell doubling in the **c** direction from α to FC26, and half of its coordination sphere resembles the α form, while the other half has the β structure. The results are an improvement over previous prediction studies for *p*-dichlorobenzene. A crystal structure prediction study[57] using the UNI model potential[91] found the γ and β polymorphs as third and fourth lowest in energy, while the α form was not located in the search, which was restricted to centrosymmetric space groups. Very recently, van Eijck[19] performed a search in five common space groups ($P1$, $P\bar{1}$, $P2_1$, $P2_1/c$, and $P2_12_12_1$) using two empirical model potentials specifically parametrized for the chlorobenzenes. The γ, α, and β forms ranked seventh, eighth, second and third, fifth, first, respectively, using the two models. The latter results are about as successful as ours, but the same model potential gave mixed results for the other chlorobenzenes studied because of the limited transferability of the spherical atom model.

The observed low temperature form is the γ polymorph, which transforms to α then β with increasing temperature, with observed enthalpies of transition of 1.24 kJ/mol (γ → α) and 0.18 kJ/mol (α → β).[76] The relative stabilities of the α and β forms are reproduced very well (Table 5). However, at the lattice energy minimum, the γ form is predicted to be less stable than both the higher temperature forms. The energy error which reverses these stabilities is very small and could well be related

(90) The heat capacity of monochlorobenzene has also been measured, but we are not confident in the relative volumes of the reported structures at different temperatures so cannot make the correction from C_V to C_P.

(91) Filippini, G.; Gavezzotti, A. *Acta Crystallogr.* **1993**, *B49*, 868.

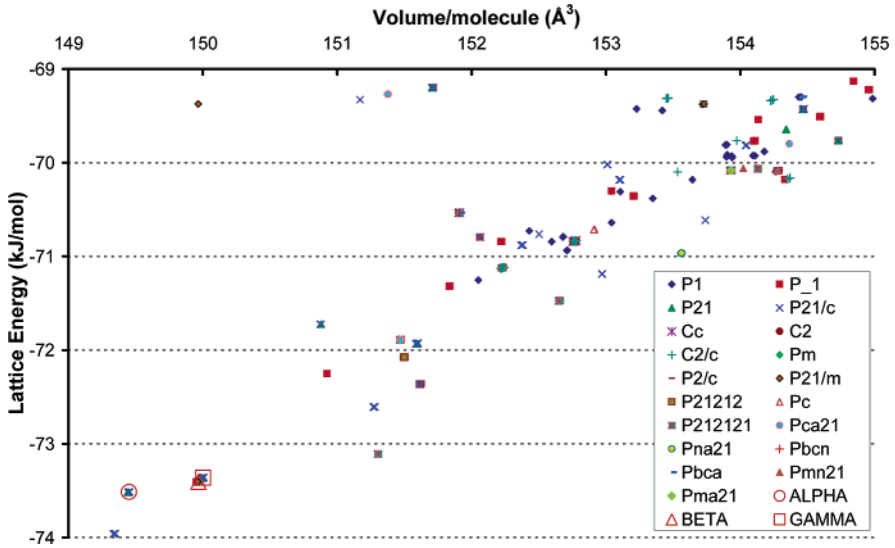

Figure 6. Lowest energy predicted structures of *p*-dichlorobenzene. The minima corresponding to the observed α, *β*, and *γ* structures are indicated by red open symbols.

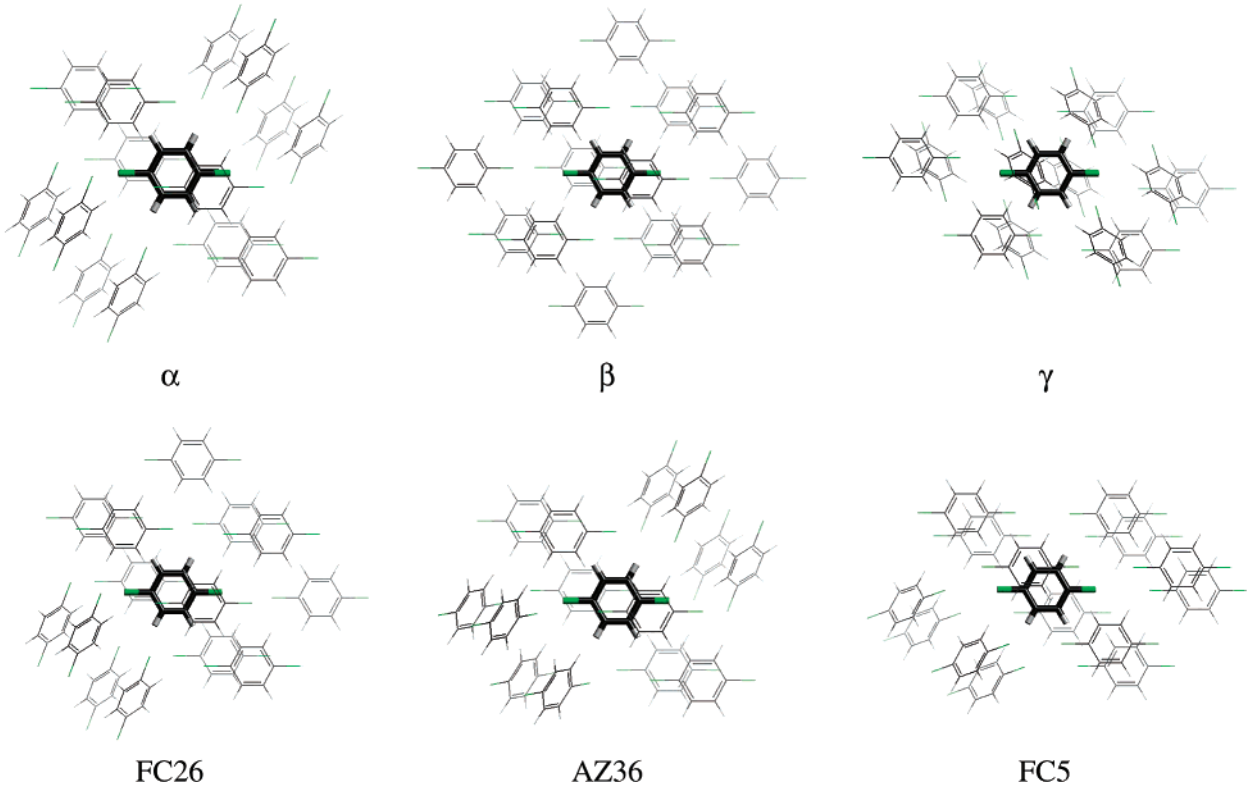

Figure 7. Coordination spheres of the six lowest energy *p*-dichlorobenzene structures found in the lattice energy search, contrasting the packing of the three known polymorphs with the three hypothetical structures.

to the apparent distortion of the molecule in the low temperature *γ* polymorph, revealing a limitation of the rigid-body approach that we have adopted.

In crystal structure prediction studies of other molecules,[92−94] additional properties, such as elastic constants and growth rates, have distinguished between the low energy structures. We examined these properties for the 13 distinct crystal structures within a 2.5 kJ/mol cutoff (Table 5). In this case, none of the low energy structures have particularly weak shear planes that might indicate crystal instability. The growth rate predictions (Table 5) are more interesting, predicting that the three known structures have significantly faster growth rates than the lowest energy predicted crystal, and indeed, they are among the fastest growing of any of the lowest energy crystals.

Discussion

The final model potential scheme, based on an accurate distributed multipole electrostatic model and a transferable atom−atom repulsion−dispersion potential with anisotropy in the repulsion, has reproduced a wide range of properties of the

(92) Beyer, T.; Day, G. M.; Price, S. L. *J. Am. Chem. Soc.* **2001**, *123*, 5086.
(93) Anghel, A. T.; Day, G. M.; Price, S. L. *CrystEngComm* **2002**, *4*, 348.
(94) Lewis, T. C.; Tocher, D. A.; Day, G. M.; Price, S. L. *CrystEngComm* **2003**, *5*, 3.

Table 5. Structures, Energies, and Relative Growth Rates of the Lowest Energy *p*-Dichlorobenzene Structures[a]

structure	space group	lattice parameters				ρ (g/cm^3)	Φ_{latt} (kJ/mol)	relative growth rate
		a (Å)	*b* (Å)	*c* (Å)	β (deg)			
FC26	$P2_1/c$	3.94	5.69	26.91	98.4	1.635	−73.96	1
AKi14 (α)	$P2_1/a$ ($Z' = {}^1/_2$)	3.97	5.62	13.54	98.6	1.633	−73.52	2.04
ABi1 (β)	$P\bar{1}$ ($Z' = {}^1/_2$)	3.87	5.86	6.70	$\alpha = 85.4$ $\beta = 82.2$ $\gamma = 88.2$	1.628	−73.40	1.71
AMi21 (γ)	$P2_1/c$ ($Z' = {}^1/_2$)	7.03	6.19	7.39	111.1	1.627	−73.36	2.10
AZ36	$P2_12_12_1$	3.95	5.70	26.89	90	1.613	−73.11	0.89
FC5	$P2_1/c$	5.86	3.91	26.39	90.5	1.614	−72.61	0.82
FA24	$P2_1/c$	3.90	27.30	5.70	92.1	1.610	−72.36	0.80
DC40	$P\bar{1}$ ($Z' = 2$)	9.61	9.73	13.32	$\alpha = 101.6$ $\beta = 97.7$ $\gamma = 90.9$	1.617	−72.25	0.58
BB16	$P2_12_12$	5.64	27.25	3.94	90	1.611	−72.08	0.88
AMi7	$P2_1/c$ ($Z' = {}^1/_2$)	6.18	3.94	12.48	93.6	1.610	−71.93	1.77
BH7	$Pca2_1$	27.34	3.97	5.58	90	1.612	−71.89	1.03
AMi18	$P2_1/c$ ($Z' = {}^1/_2$)	5.53	4.97	11.40	105.5	1.618	−71.72	2.12
FC14	*Pnma*	17.92	9.02	3.78	90	1.599	−71.47	1.14

[a] Structures are identified by their two letter MOLPAK coordination group and structure number within that group. An "i" after the two letter code indicates a coordination group with an inversion center in the molecule and $Z' = {}^1/_2$.

chlorobenzene family of molecules. The differences between the calculated and experimental properties are likely to be predominantly due to the approximations in the theory used in the calculation (e.g., static lattice energy minimization, rigid body, and harmonic approximation) implying that no significant deficiencies in the model potential can be identified by comparison with experiment.

The model potential scheme is unlikely to be definitively accurate. The derivation of the repulsion potential by the overlap model revealed limitations in the accuracy of the transferability assumption. Assuming the relationship between the overlap and the short-range repulsion potential also introduces errors. The method of estimating the dispersion contribution has an empirical aspect, and a method of determining accurate atom−atom dispersion coefficients from ab initio calculations of the monomer wave function is clearly needed. The use of atomic polarizabilities in the Slater−Kirkwood C_6 formula, with the number of valence electrons to represent the total intermolecular dispersion, including C_8 atomic terms, is somewhat empirical but pleasingly successful in this case. The induction energy has been completely neglected, along with other minor contributions such as dispersion damping. Nevertheless, the accuracy of the variety of calculated properties over the range of chlorine-to-hydrogen ratios does suggest that transferable repulsion−dispersion potentials, plus a molecule specific accurate electrostatic model, can be remarkably effective. In the case of the chlorobenzenes, the assumption that the atom−atom potential is isotropic appears to be a much greater limitation than sensible transferability assumptions in developing sufficiently accurate model potentials for molecular modeling. Fortunately, the increasing power of computers and the availability of computer programs that can handle anisotropic potentials for molecular dynamics (DL_MULTI[95] and TINKER[96]), crystal lattice energy calculations (DMAREL[64,65]), and clusters and surfaces (ORIENT[52]) mean that anisotropic potentials can be used in an increasing range of applications.

Conclusions

The chlorobenzenes are an apparently simple family of molecules whose solid-state properties have proved a major challenge to computer simulation using traditional transferable isotropic atom−atom potentials. We believe that this is the first transferable model potential scheme that can be used to predict the crystal structures, energies, and second derivative properties across the range of molecules and their polymorphs. The key feature is the development of a transferable anisotropic repulsion model, which represents the effects of the lone pair density on the intermolecular contacts. The method of developing the model potential is based on using the ab initio charge distributions of the isolated molecules, which allows the form of the anisotropy to be established and quantified and the transferability to be considered. Thus the methodology can be applied to derive model potentials from other small organic molecules and transferred to simulating the intermolecular potentials of large organic molecules. The transferable atom−atom model potential will be essential for computational studies of the condensed phases of organic molecules, such as crystal structure and polymorph prediction or molecular dynamics simulations of liquids, for many decades to come. This study on the chlorobenzenes suggests that the introduction of anisotropic repulsion for exposed nonspherical atoms can considerably increase the reliability and realism of such simulations.

Acknowledgment. G.M.D. thanks the Natural Sciences and Engineering Research Council of Canada, University College London Graduate School, and the Chancellors and Principals of the Universities of the United Kingdom (Overseas Research Scheme) for financial support.

Supporting Information Available: (S1) Further notes on the method used to parameterize the model overlap. (S2) Analysis of tranferability and the importance in the derivation of the atom−atom model for the overlap. (S3) Notes on the derivation of the dispersion parameters. (S4) Quantification of the relationship between the repulsion and model overlap. (S5) Tests of the reproduction of crystal structures and properties for various model potentials. (S6) The full calculated $\mathbf{k} = 0$ lattice mode spectrum for 1,3,5-trichlorobenzene.

JA0383625

(95) Leslie, M. L. *Mol. Phys.* Submitted.
(96) Ponder, J. *TINKER*, 4.0 ed.; Washington University, 2003.